



SU(3) Content of the Pomeranchuk Singularity*

C. QUIGG[†] and E. RABINOVICI
Fermi National Accelerator Laboratory, Batavia, Illinois 60510

ABSTRACT

The SU(3) structure of isoscalar, even signature meson exchange amplitudes in elastic meson-baryon scattering is explored. The forward amplitudes corresponding to singlet and octet exchange exhibit complicated energy dependences, neither of which can be ascribed to the exchange of a single Regge pole with an energy-independent intercept. A contribution identified with Pomeron exchange is isolated. It corresponds to a Regge pole with intercept above one. A description in terms of a mostly-singlet Pomeron and an ideally mixed f^0 trajectory gives an excellent account of total cross sections from 6 to 280 GeV/c. For $t < 0$, the singlet amplitude becomes increasingly dominant over the octet amplitude.

[†]A. P. Sloan Foundation Fellow. Also at Enrico Fermi Institute, University of Chicago, Chicago, Illinois 60637.



I. INTRODUCTION

From the time it was postulated to explain the constancy of total cross sections, the Pomeron Regge pole has been an enigma. It has always seemed mysterious that so manifestly an s-channel phenomenon as shadow scattering should admit an economical t-channel description. The unique role of the Pomeron in finite-energy-sum-rule duality¹ still awaits explanation, and it remains to be understood why total cross sections should be approximately constant. Although theoretical efforts continually have been directed toward elucidating the nature of high-energy diffraction,² only since the discovery³ that total cross sections increase at energies of several hundred GeV has the problem of the Pomeron generally been perceived as pressing. At the present time, theoretical programs to combine the constraints of duality and unitarity⁴ appear to promise some hope of understanding diffractive phenomena at experimentally attainable energies.

An important practical obstacle to the study of the Pomeron has been the difficulty of extracting Pomeron-exchange amplitudes from experimental data. Unlike the amplitudes associated with quantum number exchange, which may be parametrized neatly as power laws in the incident momentum, the vacuum exchange amplitudes are complicated functions of the beam momentum. The vacuum exchange contributions to πN and KN total cross sections, shown in Figs. 1(a) and 2(a), are first decreasing then increasing functions of the incident momenta. The ratio of the imaginary parts of the forward amplitudes for KN and πN

elastic scattering is plotted in Fig. 3. It shows clearly that the energy dependence is significantly different for πN and KN collisions, so these amplitudes cannot be ascribed to the exchange of a simple object with straightforward factorization properties. We show these features in a different way in Figs. 1(b) and 2(b), by plotting as functions of incident momentum the effective vacuum exchange intercepts

$$\alpha_{\text{eff}}(p_{\text{lab}}) = \partial \log(A(p_{\text{lab}}, t=0)) / \partial \log(p_{\text{lab}}), \quad (1)$$

where $A(p_{\text{lab}}, t=0)$ is the imaginary part of the forward elastic scattering amplitude. The effective intercepts rise from about 0.9 at low energies to values above one; they are somewhat different in πN and KN collisions.

The conventional interpretation in terms of a Pomeron (usually assumed to be approximately an $SU(3)$ singlet) with intercept near one and an f^0 Regge pole with intercept near $\frac{1}{2}$ satisfactorily accounts for the experimental information. However, it renders ambiguous the extraction of the Pomeron contribution to any process at finite energies, and raises additional questions. For example, if the Pomeron and f^0 are completely distinct objects, why should πN and KN cross sections behave so similarly with energy? Why are the relative strengths of spinflip and nonflip couplings of Pomeron and f^0 so nearly the same?⁶ The f -coupled

Pomeron scheme answers the second question (by construction), and predicts an energy-independent ratio of the vacuum contributions to πN and NN scattering which is in reasonable agreement with experiment [see Fig. 4].

Recently, Chew and Rosenzweig⁸ have made the suggestion that the Pomeron and f^0 constitute a single, chameleonic object. Over a limited range in energy, it behaves like a simple Regge pole, but the trajectory and the SU(3) structure of the coupling are energy-dependent. The more numerous the degrees of freedom which may be excited at a particular energy, the higher will be the intercept of the vacuum pole generated by multiparticle unitarity.⁹ By this interpretation, if the f^0 trajectory does not have a separate existence, it is no longer required to explain why its couplings resemble those of the Pomeron.

Stimulated by this suggestion and by the recent appearance of new data on meson-baryon scattering at high energies, we have reexamined the evidence for two vacuum poles by performing an SU(3) decomposition of the vacuum exchange amplitudes. In the next section, we describe our investigation of the forward amplitudes as measured in total cross section experiments. We identify two elements of the vacuum exchange amplitudes, a Pomeron which has a fixed power-law behavior and an ideally mixed f^0 trajectory. This differs from the classical solution of Regge pole phenomenology only in the intercept (here above one) of the Pomeron. We are not able to exclude the chameleon interpretation, but we do not find in the Chew-Rosenzweig proposal any natural interpretation of the

regularities of the data. In Section III we use techniques similar to those of Davier and Harari¹⁰ to separate the SU(3) singlet and octet contributions to nonforward vacuum amplitudes. For negative values of t , the singlet contribution becomes increasingly dominant. By a similar device we extract a "purely Pomeron" contribution to elastic scattering, and discuss its properties. Summary remarks and suggestions for further experimental investigation appear in a concluding section.

Our preferred interpretation of meson-baryon total cross sections has much in common with a long succession of Regge pole analyses. The principal novelty here is the manner in which we have manipulated the data to make apparent the properties of the individual contributions. As in all phenomenology, uniqueness is in the eye of the beholder.

II. TOTAL CROSS SECTIONS

This section is devoted to a study of the elastic amplitude at $t = 0$. We concentrate on meson-baryon scattering because the measurements in many channels permit the isolation of the vacuum exchange amplitude and the determination of its SU(3) composition.

The vacuum exchange amplitudes for πN and KN elastic scattering may be written as

$$\begin{aligned} A_{\pi N} &= S + 2O \\ A_{KN} &= S - O \quad , \end{aligned} \tag{2}$$

where S and O are amplitudes corresponding to SU(3) singlet

and octet exchange in the t-channel, respectively, and the optical theorem connection is

$$\sigma_t(p) = \text{Im } A(p, t=0) / [s - (M + \mu)^2]^{\frac{1}{2}} [s - (M - \mu)^2]^{\frac{1}{2}} \quad (3)$$

where $\mu(M)$ is the meson (nucleon) mass. We isolate the singlet and octet contributions as

$$\begin{aligned} S &= (2A_{KN} + A_{\pi N})/3. \\ O &= (A_{\pi N} - A_{KN})/3. \end{aligned} \quad (4)$$

The singlet and octet contributions to the total cross sections are shown in Figs. 5(a) and 6(a). Both of these have complicated energy dependences. The effective intercept of the singlet contributions shown in Fig. 5(b), increases from about 0.85 at 6 GeV/c to 1.05 at 280 GeV/c, while the effective intercept of the octet piece, shown in Fig. 6(b), increases from 0.6 to 1 over the same range of energies.

A third linear combination of amplitudes is also of particular physical interest. This is the combination

$$L = 2A_{KN} - A_{\pi N} = S - 4O \quad (5)$$

which eliminates the contribution of an ideal mixture of octet and singlet. According to the conventional Regge pole phenomenology, L should be free of any contribution from the f^0 trajectory: it should receive contributions only from the Pomeron. In the language of the quark model, L is the

amplitude for ϕN scattering. The contribution of L to total cross sections is shown in Fig. 7. It rises monotonically from 6 to 280 GeV/c,¹¹ and is extremely well described by a power-law in p_{lab} :¹²

$$\text{Im } L(p_{lab}, t=0) = (20.620 \text{ mb.} - \text{GeV}^2) \left[p_{lab} / (1 \text{ GeV/c}) \right]^{1.0755} \quad (6)$$

The conclusion we wish to draw from this result is that it corresponds to a simple J-plane structure with fixed intercept. It further indicates that any nonleading contribution to meson-baryon total cross sections carries the quantum numbers of an ideally mixed f^0 . The power-law fit determines the Pomeron intercept and the combination of Pomeron couplings ($P_1 - 4P_8$), in the context of standard Regge pole phenomenology. Its only unconventional aspect is the intercept above one which of course cannot persist to arbitrarily high energies. It is not natural, according to the model of Chew and Rosenzweig, to expect any total cross section to be increasing already below 30 GeV/c. On the other hand, the combination (5) is of no special significance in their model, so its remarkable energy dependence may be dismissed as accidental.

Having isolated the contribution of the putative Pomeron by eliminating any from an ideally mixed f^0 trajectory, we now carry out a two pole fit to the singlet and octet amplitudes. We have three additional parameters, namely two couplings P_1 and $f_1 = 4f_8$ and the intercept $\alpha_f(0)$. A χ^2 - fit to the data in Figs. 5 and 6 selects the values

$$\begin{aligned}
 P_1 &= 25.861 \text{ mb.} \cdot \text{GeV}^2, \\
 P_8 &= 1.310 \text{ mb.} \cdot \text{GeV}^2, \\
 f_1 &= 43.507 \text{ mb.} \cdot \text{GeV}^2, \\
 \alpha_f(0) &= 0.4081, \qquad (7)
 \end{aligned}$$

where P_8 has been determined using Eq. (6). The resulting excellent fits are those shown in Fig. 5(a) and 6(a). The consequential parametrizations of the physical processes are the solid curves in Figs. 1(a) and 2(a). The quality of these fits is superior, even over a limited energy regime, to the one vacuum pole fits by Bali and Dash,⁸ which are often cited as support for the conjecture that the Pomeron and f^0 are the same object. It may be remarked that the fitted value of the f^0 -intercept is in close agreement with measured values of the ω -intercept (of which more below) and with the value deduced from the meson spectrum under the assumption of ω - f^0 exchange degeneracy. We are therefore justified in interpreting the non-Pomeron component of vacuum exchange amplitudes as that of the f^0 -trajectory. In the model of Chew and Rosenzweig, the f^0 -like character of the nonleading contribution is, like the energy dependence of the " ϕ N" cross section, unexpected.

The relative strength of the octet coupling of the Pomeron is here determined quite reliably, principally because of the very high energy data available to us. The ratio $P_8/P_1 = 0.05$

is in reasonable agreement with the fraction of approximately 0.08 suggested by the f-coupled Pomeron model.⁷ It exceeds by roughly a factor of two the two-pion exchange octet coupling estimated by Kane and Pumplin.¹³

The celebrated flatness of K^+ nucleon total cross sections is simply explained in traditional Regge phenomenology, in which the Pomeron exchange contribution is energy-independent. The imaginary parts of the f^0 - and ω -exchange amplitudes cancel, as prescribed by duality or exchange degeneracy, leaving only the constant Pomeron contribution. How does the description now under discussion achieve such flatness? The ω -exchange contribution can be determined by fitting the amplitude

$$\Omega = \frac{1}{4} \begin{bmatrix} A & + A & - A & - A \\ K^+p & K^+n & K^-p & K^-n \end{bmatrix} \\ \approx (-13.758 \text{ mb.} - \text{GeV}^2) (p_{\text{lab}}/(1 \text{ GeV}/c))^{0.4487} \quad (8)$$

The fitted ω -intercept is a reasonable one. Fits to $K^\pm d$ and $p^\pm d$ total cross section differences both yield intercepts of 0.43. From measurements of the coherent regeneration reaction $K_L d \rightarrow K_S d$ between 12 and 50 GeV/c at Serpukhov,¹⁴ the intercept is $\alpha_\omega(0) = 0.46 \pm 0.06$. Preliminary Fermilab measurements¹⁵ of $K_L C \rightarrow K_S C$ between 30 and 120 GeV/c give a value of $\alpha_\omega(0) = 0.41 \pm 0.03$. The ω coupling in KN scattering is however considerably smaller than that (32.630 mb. - GeV^2) of the f^0 -trajectory. Hence, while the two Reggeon exchange amplitudes tend to cancel in the K^+N channel, the cancellation is

incomplete. The resultant description of K^+N total cross sections is shown in Fig. 8. The price we are forced to pay for fits with a Pomeron intercept above one is (predictably) the abandonment of strong exchange degeneracy. The phenomenological case for strong $f^0-\omega$ exchange degeneracy has always been somewhat shaky,¹⁶ so this is not a radical outcome, although it is rather ungraceful.

A more speculative check of the f^0 -likeness of the secondary trajectory can be made by relating meson-baryon and baryon-baryon scattering by means of the CGZ ansatz.⁷ The test of the f -coupled Pomeron model given in Fig. 4 indicates that we may obtain a general description of NN cross sections by multiplying our parametrization of πN cross sections by a constant. In Fig. 9 we compare the measured vacuum exchange contribution to NN scattering with $1.70 \times$ the πN parametrization. The most objectionable qualitative feature of the "prediction" is its tendency to rise at energies where the NN data remain flat. Other authors,¹⁷ unconstrained by the f -coupling scheme, have succeeded in fitting the ISR measurements³ of $\sigma_t(pp)$ with a Pomeron intercept near 1.07, but the flatness of the cross section between 100 and 300 GeV/c is difficult to reproduce in a two pole model.

It is important to discuss the implications of the unconventional attribute of our two-pole description, namely the Pomeron intercept above one. The Froissart bound prohibits

the persistence of such behavior to asymptotic energies, so we must ask whether over the range of energies we have explored a power-law growth is conceivable. The relevant criterion for the onset of unitarity corrections is not the value of the pole intercept, but the magnitude of partial wave amplitudes. Preliminary analyses¹⁸ of meson-baryon elastic scattering between 50 and 175 GeV/c indicate that the partial wave amplitudes at zero impact parameter still lie far below the rigorous unitarity bound, and probably also well below the effective bounds incorporating models for diffraction dissociation.¹⁹ Coupled with the absence of pronounced diffraction minima for moderate values of t , this indicates that absorptive effects are unimportant in the meson-baryon sector in the energy interval in which data are available.

We have also studied the effects of absorption in the context of a theoretical model. The energy dependence of an input Regge pole amplitude with intercept at 1.08 and with a $b=0$ partial wave of the order encountered in meson-baryon scattering is changed only slightly by application of the Gottfried-Jackson absorption prescription.²⁰ The effective intercept is lowered by less than 0.01 over the entire energy range we consider. Although this exercise is quite schematic, we believe it explains the compatibility of an energy-independent singularity above one with the data. For the larger partial-wave amplitudes appropriate to NN scattering, our model

calculation leads us to expect a somewhat larger quenching of the Pomeron intercept (by about 0.015) which would again be virtually independent of energy up to 300 GeV/c. These differences in the expected unitarity corrections are likely to complicate relationships between meson-baryon and baryon-baryon scattering.

We note that Collins, et al., and Capella, et al.²¹ have published descriptions of meson-baryon total cross sections which include a Pomeron with intercept near 1.1. While they have not been concerned with the SU(3) structure and systematics of vacuum exchanges as we have, their fitted parameters bear some resemblance to ours.

Lipkin¹¹ has made a detailed study of deviations from the additive quark model in meson-proton and baryon-proton total cross sections, enforcing the constraints of strong f^0 - ω exchange degeneracy. He found a number of remarkable connections between meson-baryon and baryon-baryon cross sections which led him to identify a non-singlet component of the Pomeron. The new component was parametrized as a pole below one. Within the meson-baryon sector and free from strong f^0 - ω exchange degeneracy, we see no indication that the Pomeron octet must be assigned to a new J-plane singularity. Indeed, the effective octet intercept displayed in Fig. 6(b) argues against an intercept much below one.

III. NONFORWARD ELASTIC AMPLITUDES

We report here the results of an exploratory study of the SU(3) content of vacuum exchange amplitudes away from the forward direction. This natural extension of our analysis at $t=0$ is given impetus by the experimental observation²² that at Fermilab energies the differential cross sections for πN and KN scattering approach each other for $t < 0$ and by the theoretical suggestion²³ that the SU(3) singlet part of the Pomeron amplitude should become dominant over the octet part for $t < 0$. Our aim is to begin to quantify the experimental result and to compare it with these speculations.

In the absence of high-energy amplitude analyses it is necessary to make a number of technical assumptions to draw inferences about the properties of amplitudes. Our technique will parallel the one introduced by Davier and Harari¹⁰ to study the structure of quantum number exchange amplitudes. We assume that only a single spin amplitude is important, and write

$$\frac{d\sigma}{dt} (\pi^\pm p) = |\Pi_+ \pm \Pi_-|^2, \quad (9)$$

$$\frac{d\sigma}{dt} (K^\pm p) = |K_+ \pm K_-|^2, \quad (10)$$

where Π_\pm and K_\pm are the $C = \pm 1$ exchange amplitudes for πN and KN scattering. We form the combinations

$$\begin{aligned} \frac{1}{2} \left[\frac{d\sigma}{dt} (\pi^+ p) + \frac{d\sigma}{dt} (\pi^- p) \right] &= \left\{ |\Pi_+|^2 + |\Pi_-|^2 \right\} \\ &\approx |\Pi_+|^2 \end{aligned} \quad (11)$$

and

$$\frac{1}{2} \left[\frac{d\sigma}{dt}(K^+p) + \frac{d\sigma}{dt}(K^-p) \right] = \left\{ |K_+|^2 + |K_-|^2 \right\} \\ \approx |K_+|^2, \quad (12)$$

neglecting the odd-signature contributions compared to those of even signature, an excellent approximation at 50 GeV/c and above. The only even signature contribution to πN scattering is from vacuum exchange, so we identify

$$|V_\pi|^2 = \frac{1}{2} \left[\frac{d\sigma}{dt}(\pi^+p) + \frac{d\sigma}{dt}(\pi^-p) \right]. \quad (13)$$

For $K^\pm p$ scattering, K_+ contains both vacuum and A_2 -exchange contributions. The latter cannot be eliminated without information on $K^\pm n$ elastic scattering. At the energies of interest, we know from total cross section data that the A_2 contribution may safely be neglected at $t=0$. Although we cannot justify neglecting it for $t<0$, we must do so to proceed. Therefore, we write

$$|V_K|^2 \approx \frac{1}{2} \left[\frac{d\sigma}{dt}(K^+p) + \frac{d\sigma}{dt}(K^-p) \right]^2. \quad (14)$$

We are now ready for the SU(3) decomposition. We write

$$|V_\pi|^2 = |S + 2O|^2 \approx |S|^2 + 4 \operatorname{Re} S^* O, \\ |V_K|^2 = |S - O|^2 \approx |S|^2 - 2 \operatorname{Re} S^* O, \quad (15)$$

where the t -dependence of the singlet and octet amplitudes S and O is implicit.²⁴ The combinations

$$|S|^2 = (2|V_K|^2 + |V_\pi|^2)/3 \quad (16)$$

and

$$O_{\parallel} = \frac{|V_\pi|^2 - |V_K|^2}{6|S|} \quad (17)$$

isolate the differential cross section arising from singlet exchange and the octet amplitude in phase with the singlet amplitude. The smallness of O_{\parallel} will demonstrate that it is consistent to neglect the $|O|^2$ terms in Eq. (15).

The singlet contribution to meson-baryon scattering between 50 and 200 GeV/c is shown in Fig. 10. It has approximately an exponential dependence upon t , and there is a hint of shrinkage. The octet exchange amplitude (in phase with the singlet exchange) is plotted in Fig. 11. It falls off very rapidly with t , and is consistent with zero for $t < -0.4$ (GeV/c)². This shows quantitatively the increasing dominance of singlet exchange over octet exchange away from the forward direction. A number of interesting questions cannot be answered with the available data. We should like to decompose the nonforward amplitudes into Pomeron and f^0 contributions as we did in Figs. 5 and 6 at $t=0$ by fitting the energy dependence for each value of t . From this exercise we would learn whether the octet part of the Pomeron amplitude is peripheral. Similar exercises can be carried out in impact parameter space.

Although we cannot demonstrate with data over only a limited range of energies that

$$|L|^2 = |S - 40|^2 \approx 2|V_K|^2 - |V_\pi|^2 \quad (18)$$

has single Regge pole behavior for $t < 0$, as it does at $t=0$, it is of interest to ask whether this combination indeed has the properties we expect of pure Pomeron exchange. Its contribution to elastic meson baryon scattering^{2 5} is shown in Fig. 12. It is exponential in t , and shrinks in a manner compatible with a moving trajectory with about half-normal slope. Although no firm conclusion can be drawn from these data, it is comforting that the trajectory appears to be a reasonable one.

Our analysis indicates that the importance of the octet contribution to the vacuum exchange amplitude for meson-baryon elastic scattering diminishes rapidly away from $t=0$. This behavior is compatible with the conjecture of Chew and Rosenzweig and with the hypothesis that the octet part of the Pomeron is peripheral. We are not able to separate Pomeron and f^0 contributions using the data in hand. We are hopeful that the extension of this kind of analysis to lower energies, with due attention to the problem of A_2 exchange in $K^\pm p$ scattering, will yield more definitive results. The answer to the long-standing question of the peripherality of tensor exchanges may be found in this way. Additional measurements of the differential cross section for ϕN elastic scattering, which according to the quark model is equal to the "pure Pomeron" contribution L , will provide another source of information

on the Pomeron amplitude for $t \neq 0$. The importance of such measurements at Fermilab is already recognized.

IV. CONCLUSIONS

A two Regge pole parametrization gives an excellent description of the vacuum exchange contribution to meson-baryon total cross sections between 6 and 280 GeV/c. The Pomeron, which lies above one in the J-plane, is an almost pure SU(3) singlet at $t=0$. The ideally-mixed f^0 -trajectory and its partner the ω have approximately the same intercept, but the f^0 couples more strongly than planar duality would suggest. The relative signs of the f^0 and ω couplings agree with the requirements of exchange degeneracy.

In the framework of theoretical models, the structure of the Reggeon field theory and of s-channel absorption models is potentially very rich when the bare Pomeron intercept lies above one. Over the currently accessible range of energies, however, unitarity effects seem not to complicate the simple Regge pole description in the forward direction.

The two vacuum pole model gives in our opinion a simpler interpretation of the total cross section data than is possible in the Chew-Rosenzweig picture. The energy dependence of the combination $2\sigma_t(KN) - \sigma_t(\pi N)$ and the ideally-mixed f^0 quantum numbers of the nonleading pole are not obvious consequences of their scheme.

We have proposed a technique for extracting (parts of) the singlet and octet vacuum exchange amplitudes in nonforward elastic scattering, and used it to quantify the dominance of singlet amplitude for $t < 0$. This element of the Chew-Rosenzweig model is in good agreement with the data. It was not possible, using data at 50 - 200 GeV/c, to make detailed statements about the energy- and t -dependence of the individual contributions to the vacuum exchange amplitudes. We anticipate that this will be a fertile area for further investigation.

ACKNOWLEDGEMENTS

We are grateful to G.F. Chew, M.B. Einhorn, R.D. Field, M. Jacob, H.J. Lipkin, U. Maor, G. Mikenberg, C. Rosenzweig, and C. Sorenson for many animated discussions.

FOOTNOTES AND REFERENCES

- ¹P.G.O. Freund, Phys. Rev. Lett. 20, 235 (1968); H. Harari, ibid., 20, 1395 (1968).
- ²F. Zachariasen, Phys. Rep. 2C, 1 (1971), T.T. Wu and H. Cheng, in High-Energy Collisions-1973, edited by C. Quigg (New York: AIP), p. 54; G.F. Chew, ibid., p. 98; H.D.I. Abarbanel, J.D. Bronzan, R.L. Sugar, and A.R. White, Phys. Rep. 21C, 119 (1975).
- ³U. Amaldi, et al., Phys. Lett. 44B, 112 (1973); S.R. Amendolia, et al., ibid., 44B, 119(1973), and Nuovo Cimento 17A, 735 (1973).
- ⁴See, for example, the talks by G. Marchesini, J. Paton, C. Rosenzweig, and C. Schmid at the VI International Colloquium on Multiparticle Dynamics, Oxford, 1975.
- ⁵W. Galbraith, et al., Phys. Rev. 138, B913 (1965); K.J. Foley, et al., Phys. Rev. Lett. 19, 330, 857 (1967); S.P. Denisov, et al., Phys. Lett. 36B, 415, 528 (1971), and Nucl. Phys. B65, 1 (1973); A.S. Carroll, et al., Phys. Rev. Lett. 33, 928, 932 (1974), and FERMILAB-Pub-75/51-EXP.
- ⁶As indicated by the near-mirror symmetry of the polarization in $\pi^{\pm}p$ elastic scattering.
- ⁷R. Carlitz, M.B. Green, and A. Zee, Phys. Rev. D4, 3439 (1971).
- ⁸C. Rosenzweig and G.F. Chew, Phys. Lett. 58B, 93 (1975). G.F. Chew and C. Rosenzweig, Berkeley preprints LBL-4201 & 4603, G.F. Chew, "Multiple Production as a Source of Insight into the Origin of Hadrons," at the Fermilab Symposium on Hadron Physics in Bubble

Chambers, September, 1975. See also N.F. Bali and J. Dash, Phys. Rev. D10, 2102 (1974).

⁹Strictly speaking, the unitarity arguments lead to predictions about the behavior of the nondiffractive inelastic cross section. The absence of precise data on the $K^{\pm}n$ elastic cross sections and on the contributions of inelastic diffraction in any channel discourages us from repeating our exercise for $\sigma_{\text{inelastic}}$.

¹⁰M. Davier and H. Harari, Phys. Lett. 35B, 239 (1971).

¹¹This has been remarked already by H.J. Lipkin, Phys. Rev. D11, 1827 (1974) for the combination $\sigma_t(K^+p) + \sigma_t(K^-p) - \sigma_t(\pi^-p)$.

¹²We quote fitted parameters to sufficient precision that the reader can reproduce our curves.

¹³J. Pumplin and G.L. Kane, Phys. Rev. D11, 1183 (1975).

¹⁴K.-F. Albrecht, et al., Berlin preprint PHE 75-7, Contribution to the EPS International Conference on High-Energy Physics, Palermo.

¹⁵Preliminary results of Fermilab experiment E82, Chicago-San Diego-Wisconsin Collaboration; B. Winstein, private communication.

¹⁶G.C. Fox and C. Quigg, Ann. Rev. Nucl. Sci. 23, 219 (1973); H. Harari, in Theories of Strong Interactions at High Energies, edited by R.F. Peierls, Brookhaven Report BNL-50212, p. 385.

¹⁷H. Cheng, J.K. Walker, and T.T. Wu, Phys. Lett. 44B, 97(1973); P.D.B. Collins, F.D. Gault, and A. Martin, Phys. Lett. 47B, 171 (1973); A. Capella and J. Kaplan, Phys. Lett. 52B, 448 (1974).

S.Y. Chu, B.R. Desai, B.C. Shen, and R.D. Field, U.C. Riverside preprint UCR-75-03, have shown that a bare Pomeron above one can also describe high-energy data on elastic and quasi-elastic pp scattering.

- ¹⁸G. Mikenberg, private communication; D. Cutts, "Elastic Scattering at FNAL," presented at X^e Rencontre de Moriond, 1975.
- ¹⁹For a discussion of augmented bounds, see H.I. Miettinen, Rapporteur Report at the EPS International Conference on High Energy Physics, Palermo, CERN Preprint TH-2072.
- ²⁰K. Gottfried and J.D. Jackson, Nuovo Cimento 34, 735 (1964).
- ²¹P.D.B. Collins, F.D. Gault, and A. Martin, Nucl. Phys. B83, 241 (1974); A. Capella, J. Tran Thanh Van, and J. Kaplan, ibid. B97, 493 (1975).
- ²²At 50, 100, and 200 GeV/c: C.W. Akerlof, et al., Phys. Rev. Lett. 35, 1406 (1975); at 50, 70, 100, 140, and 175 GeV/c: Fermilab Single Arm Spectrometer Collaboration, Phys. Rev. Lett. 35, 1195 (1975). **The data points we used differ slightly from those published by the Single Arm Spectrometer Collaboration. A final publication of that group's data will be issued shortly.**
- ²³For example, Chew and Rosenzweig, Ref. 8; Pumplin and Kane, Ref. 13.
- ²⁴The quantities S and O defined here differ by a kinematical factor from those in §II. The change should cause no confusion.
- ²⁵In the spirit of the quark model, this is a prediction for ϕN elastic scattering.

FIGURE CAPTIONS

- Fig. 1: (a) The vacuum exchange contribution to πN total cross sections $\left[\sigma_t(\pi^+p) + \sigma_t(\pi^-p) \right]$. The data are from Ref. 5. The curve is the two Regge pole fit described in Section II. (b) The effective vacuum exchange intercept for πN scattering as defined in eq. (1).
- Fig. 2: (a) The vacuum exchange contribution to KN total cross sections $\left[\sigma_t(K^+p) + \sigma_t(K^+n) + \sigma_t(K^-p) + \sigma_t(K^-n) \right]$. The data are from Ref. 5. The curve is the two Regge pole fit described in Section II. (b) The effective vacuum exchange intercept for KN scattering as defined in eq. (1).
- Fig. 3: Ratio of the imaginary parts of the vacuum exchange contributions to the forward elastic scattering amplitudes for KN and πN collisions. In the absence of a secondary vacuum trajectory, or if couplings of all vacuum trajectories were proportional, the ratio should be energy-independent. In the f -coupled Pomeron scheme, the ratio should approach the value $\left\{ \alpha_P(0) - \frac{1}{2} [\alpha_f(0) + \alpha_{f^*}(0)] \right\} / [\alpha_P(0) - \alpha_{f^*}(0)] \approx 0.8$ at high energies. The data are from Ref. 5.
- Fig. 4: Ratio of the imaginary parts of the vacuum exchange contributions to the forward elastic

scattering amplitudes for NN and πN collisions. The f-coupled Pomeron scheme predicts an energy-independent ratio. The data are from Ref. 5.

Fig. 5: (a) SU(3) singlet part of the vacuum exchange contribution to meson-baryon total cross sections. The data are from Ref. 5. The solid curve is a two Regge pole fit described in the text. The dashed line is the Pomeron contribution, the dotted line is the contribution of the ideally-mixed f^0 trajectory
(b) The effective intercept for the singlet part, defined through eq. (1).

Fig. 6: (a) SU(3) octet part of the vacuum exchange contribution to meson-baryon total cross sections. The data are from Ref. 5. The curve is a two Regge pole fit described in the text. The dashed line is the Pomeron contribution, the dotted line is the contribution of the ideally-mixed f^0 trajectory.

Fig. 7: Contribution of the "f-free" combination L , defined in eq. (5), to meson-baryon total cross sections. The data are from Ref. 5. The curve is the Pomeron Regge pole parametrization given by eq. (6).

Fig. 8: The isoscalar exchange contribution to K^+N total cross sections. The data are from Ref. 5. The curve is the three Regge pole fit described in the text. The dashed line is the Pomeron contribution; the dotted line is the contribution of f^0 and ω Regge poles.

- Fig. 9: Vacuum exchange contribution to NN total cross sections. The data are from Ref. 5 and Ref. 3. The curve, suggested by the f-coupled Pomeron model, is $1.70 \times$ the fitted vacuum exchange contribution to πN scattering. It deviates from the NN data above 150 GeV/c and would lie systematically above the ISR measurements of $\sigma_t(pp)$.
- Fig. 10: Vacuum exchange SU(3) singlet contribution to meson-baryon elastic scattering from 50 to 200 GeV/c. The data are from Ref. 22. The "optical points" are derived from the total cross section analysis of the previous section.
- Fig. 11: Octet amplitude, defined by Eq. (17), for meson-baryon elastic scattering from 50 to 200 GeV/c. The data are from Ref. 22. The "optical points" are derived from the total cross section analysis of the previous section.
- Fig. 12: "Pure Pomeron" contribution, defined by Eq. (18), to meson-baryon elastic scattering from 50 to 200 GeV/c. The data are from Ref. 22. The "optical points" are derived from the total cross section analysis of the previous section.

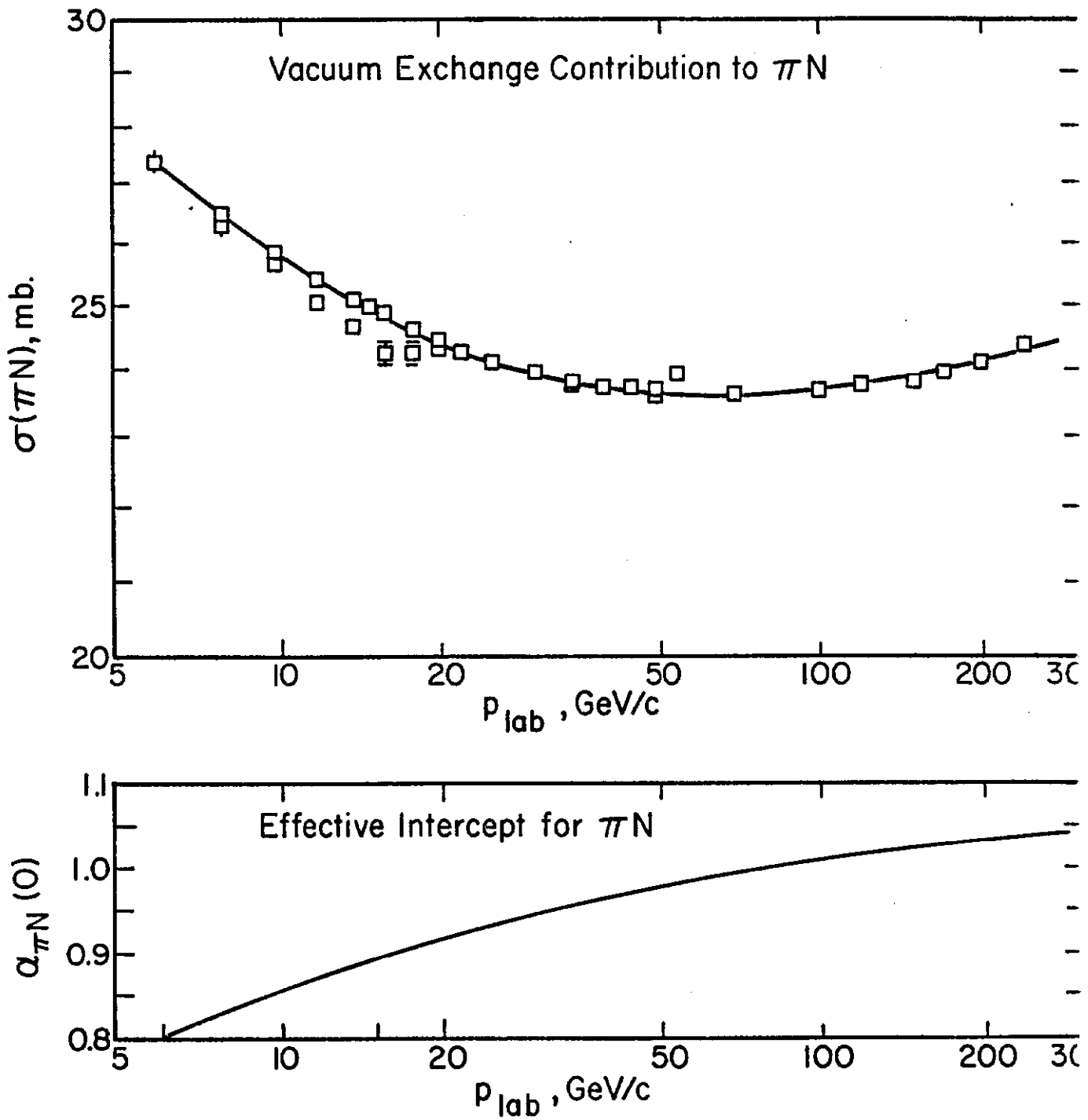


Fig. 1

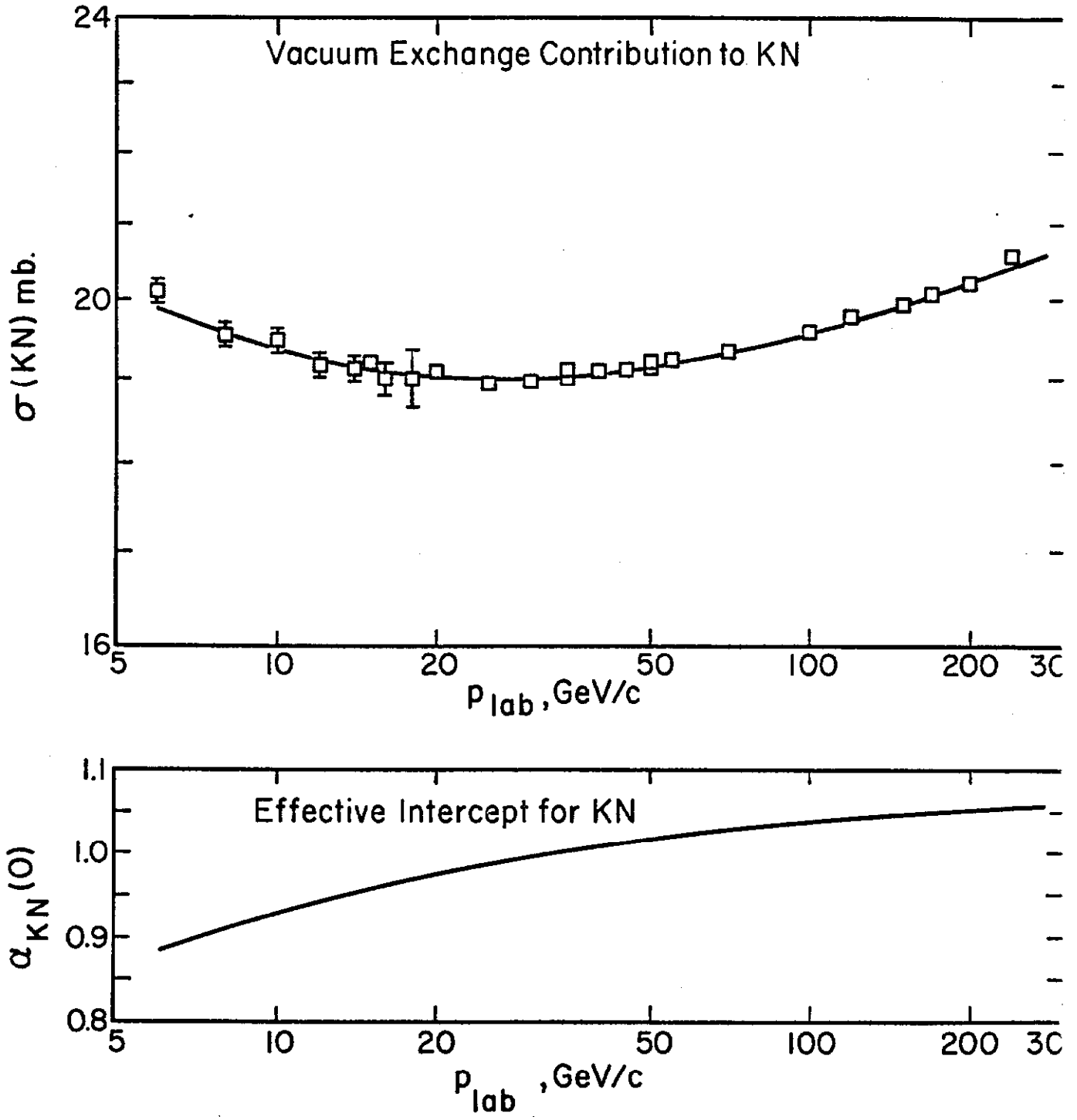


Fig. 2

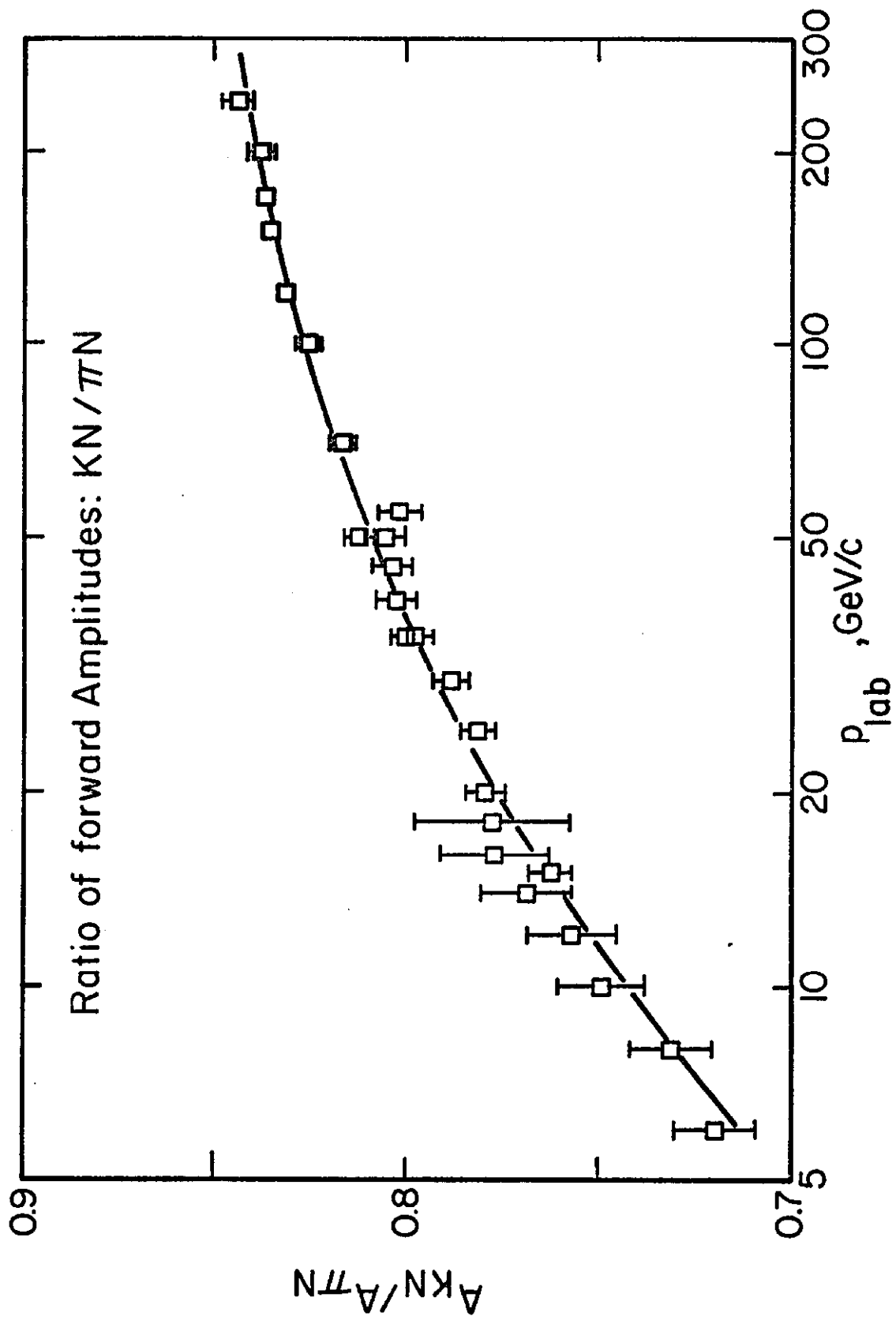


Fig. 3

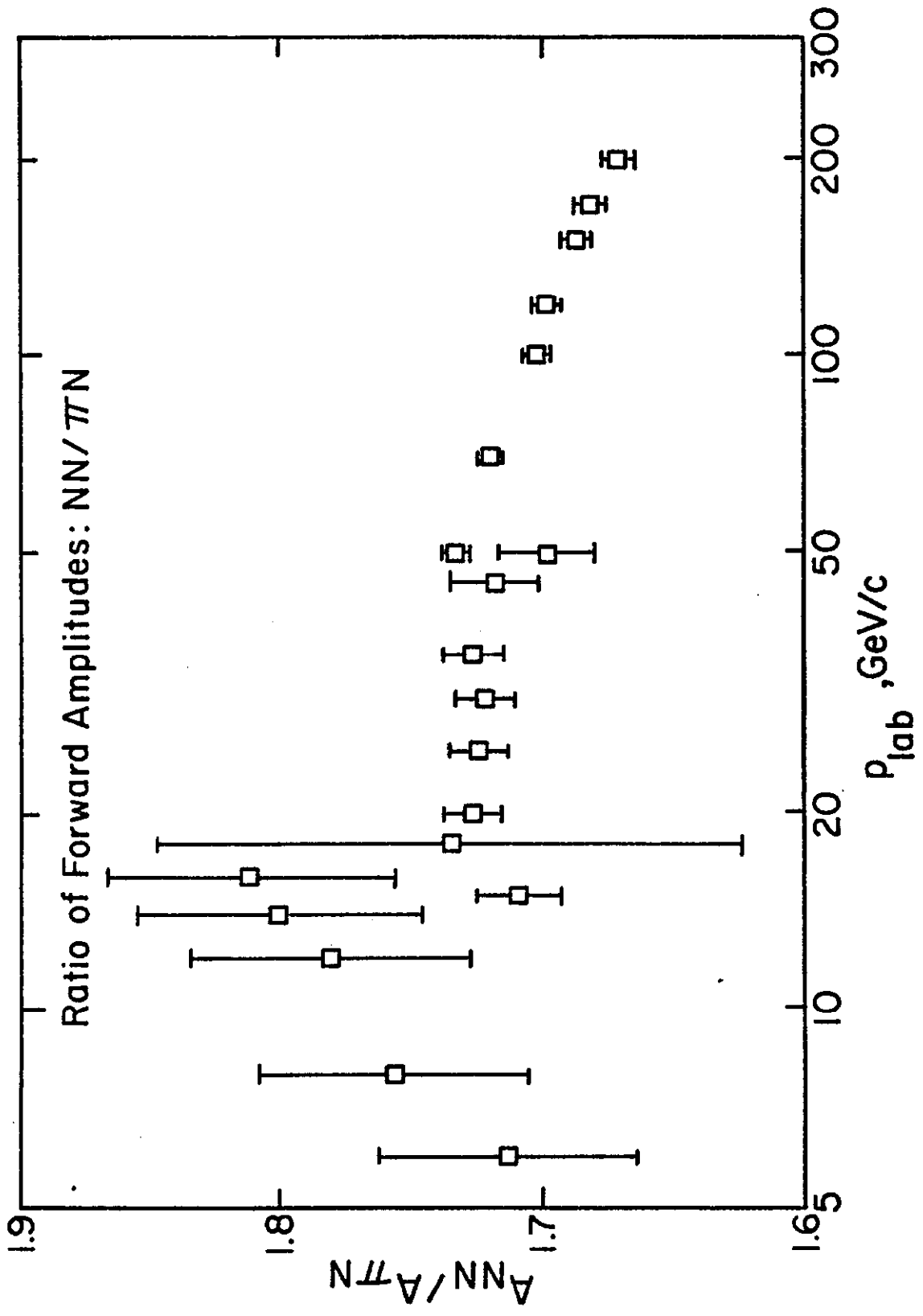


Fig. 4

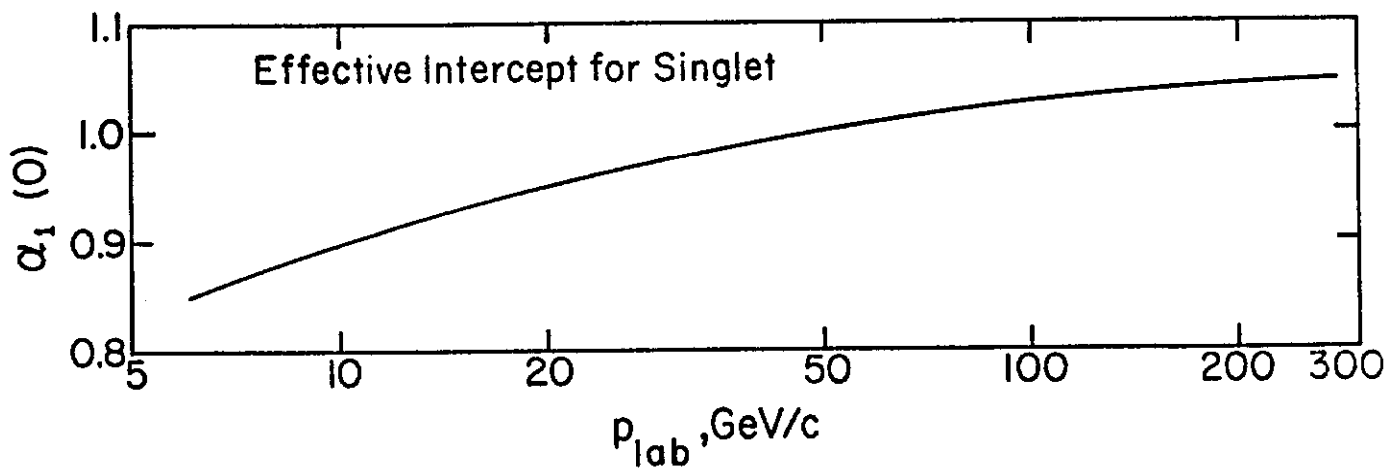
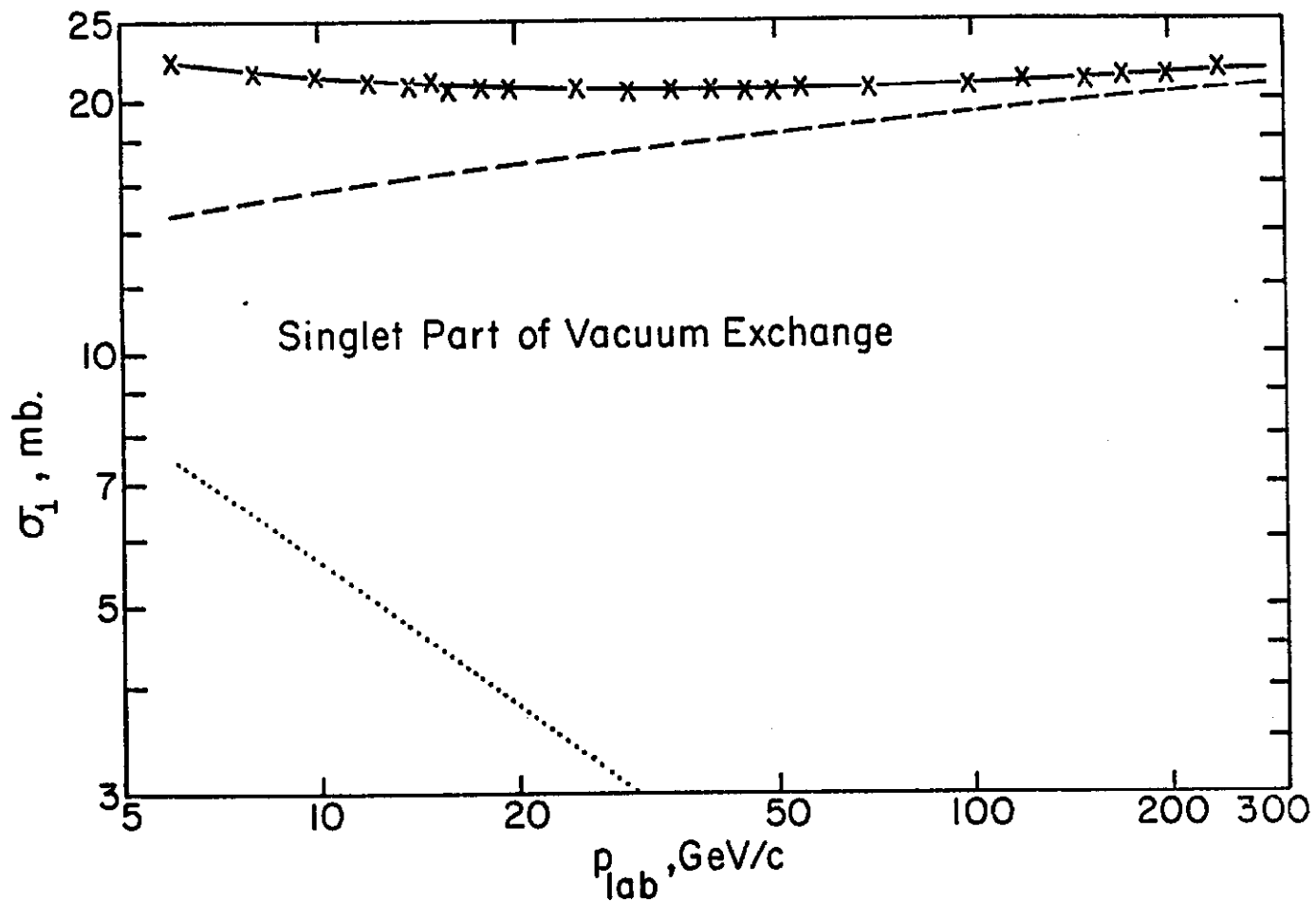


Fig. 5

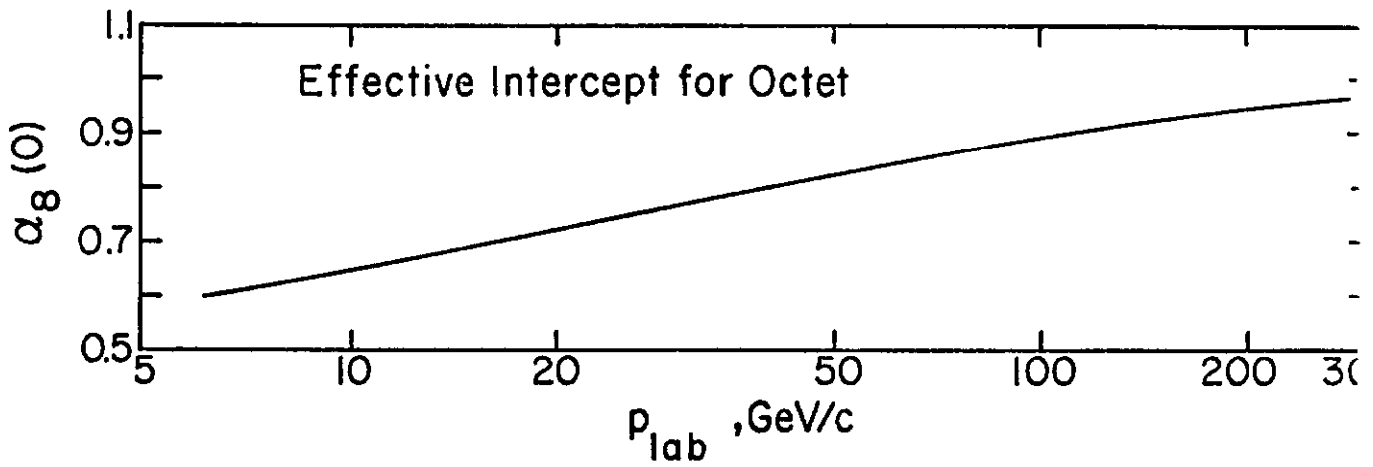
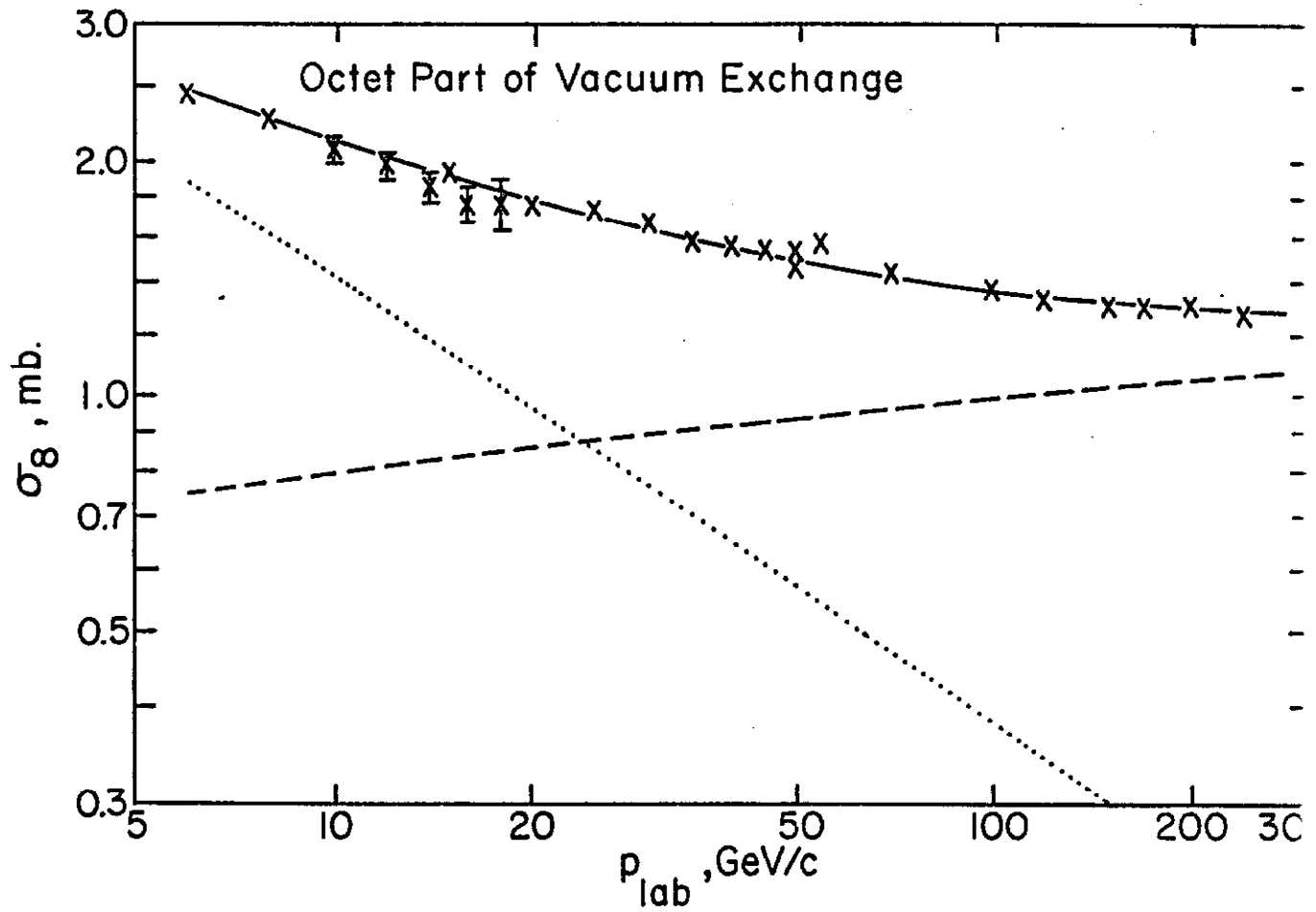


Fig. 6

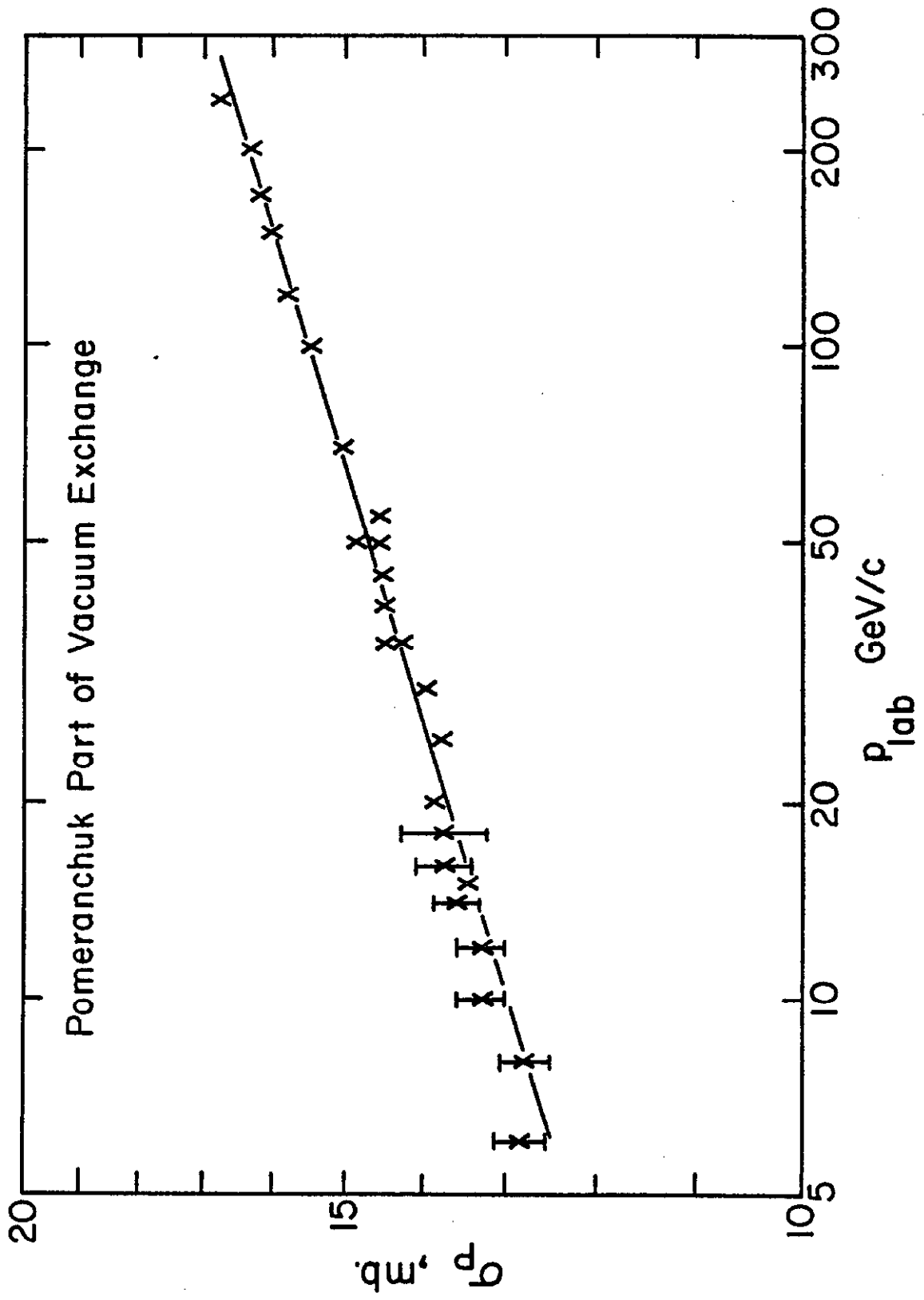


Fig. 7

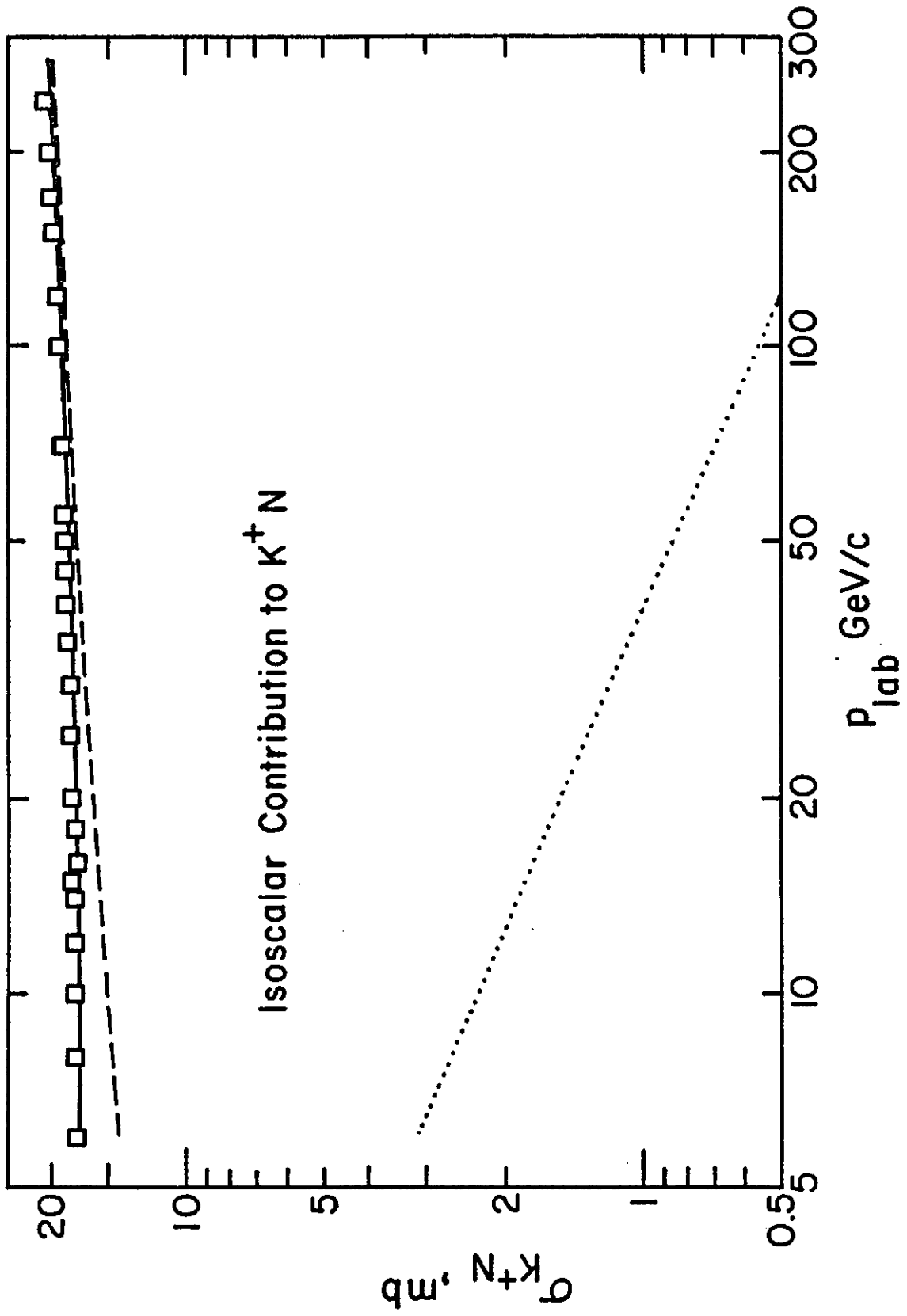


Fig. 8

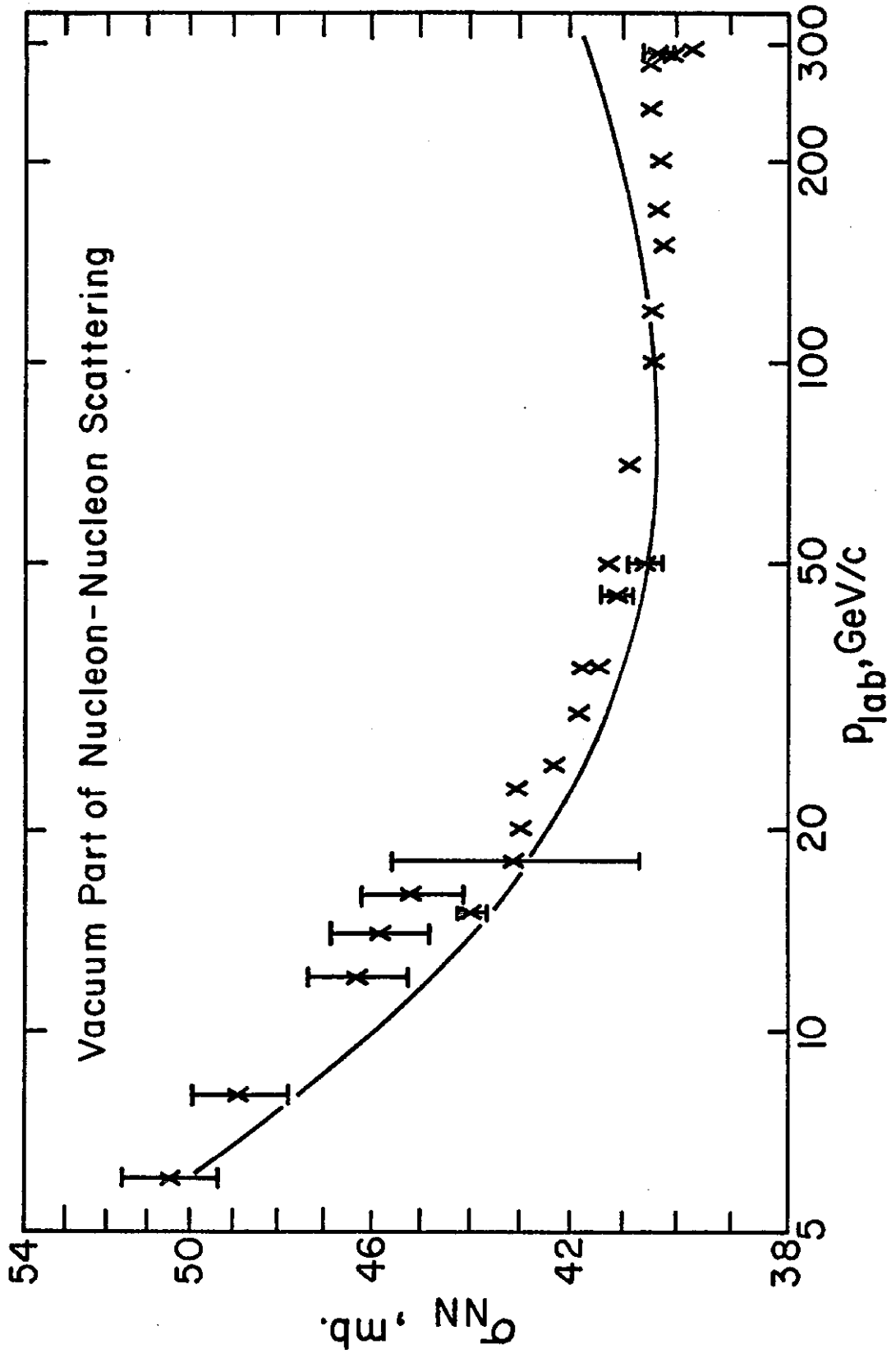


Fig. 9

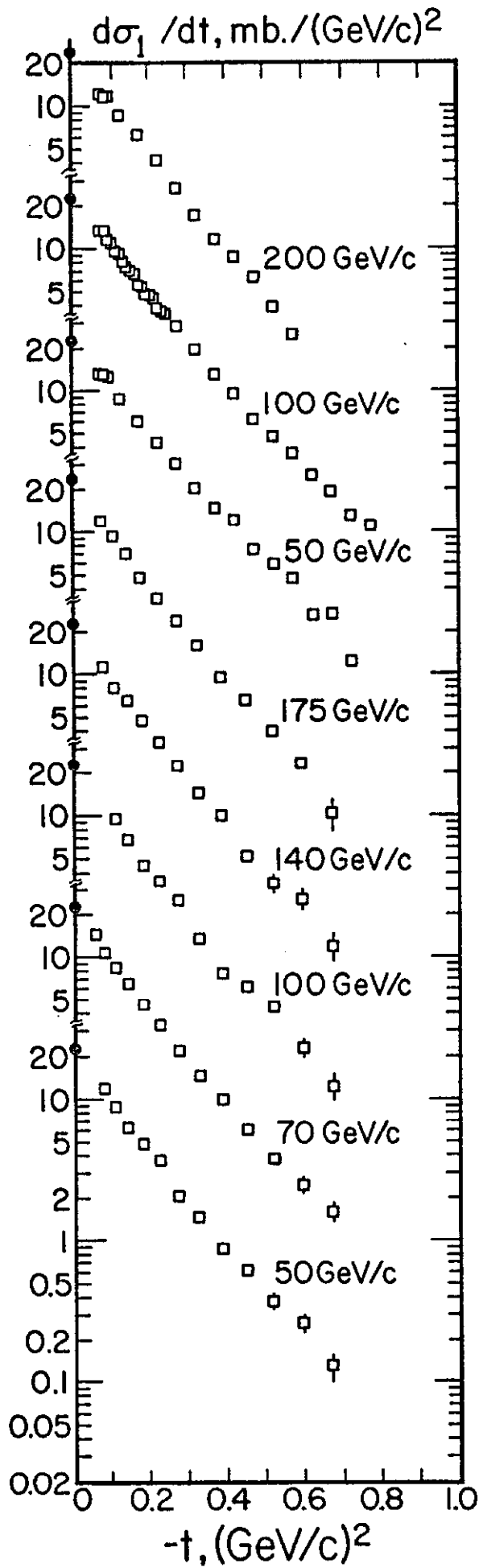


Fig. 10

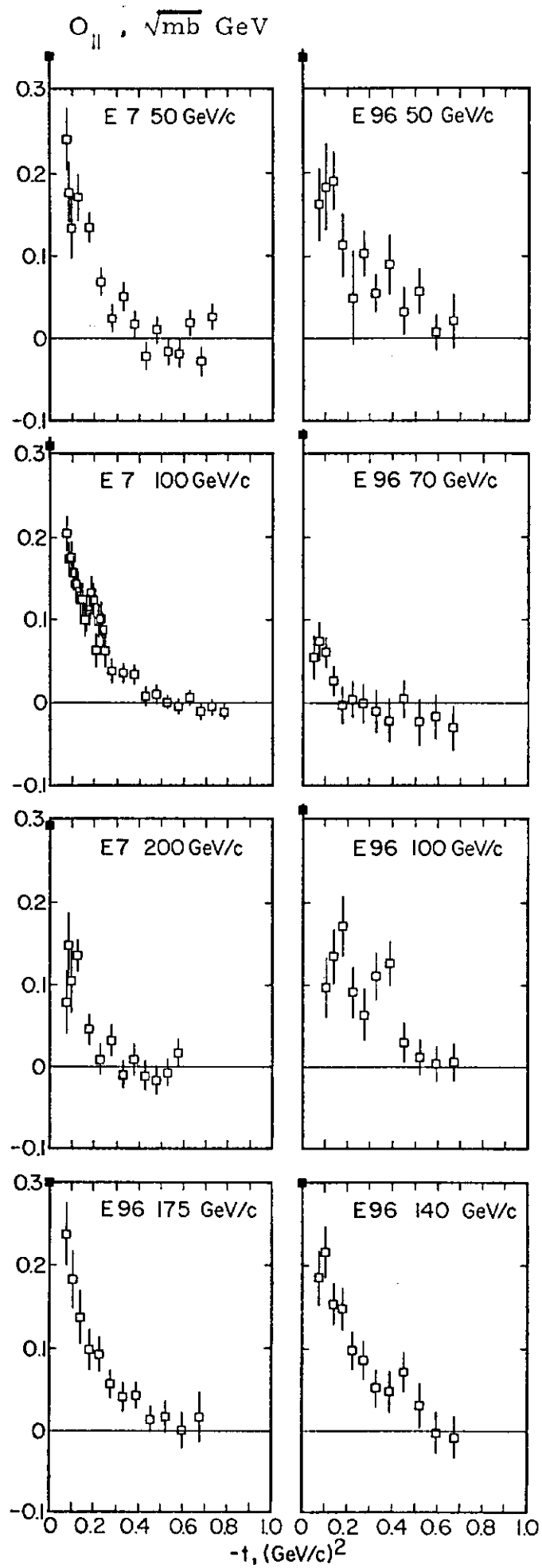


Fig. 11

Fig. 12

